AIP Advances

Electron injection-induced effects in Si-doped β-Ga_2O_3

Cite as: AIP Advances **9**, 015127 (2019); https://doi.org/10.1063/1.5079730
Submitted: 02 November 2018 . Accepted: 11 January 2019 . Published Online: 23 January 2019

Sushrut Modak, Jonathan Lee, Leonid Chernyak, Jiancheng Yang, Fan Ren, Stephen J. Pearton, Sergey Khodorov, and Igor Lubomirsky

Electron injection-induced effects in Si-doped β-Ga_2O_3

Cite as: AIP Advances 9, 015127 (2019); doi: 10.1063/1.5079730
Submitted: 2 November 2018 • Accepted: 11 January 2019 •
Published Online: 23 January 2019

View Online Export Citation CrossMark

Sushrut Modak,[1] Jonathan Lee,[1] Leonid Chernyak,[1,a)] Jiancheng Yang,[2] Fan Ren,[2] Stephen J. Pearton,[3] Sergey Khodorov,[4] and Igor Lubomirsky[4]

AFFILIATIONS

[1]Department of Physics, University of Central Florida, Orlando, Florida 32816, USA
[2]Department of Chemical Engineering, University of Florida, Gainesville, Florida 32611, USA
[3]Material Science and Engineering, University of Florida, Gainesville, Florida 32611, USA
[4]Department of Materials and Interfaces, Weizmann Institute of Science, Rehovot 76100, Israel

[a)]**Electronic addresses:** chernyak@physics.ucf.edu and Leonid.Chernyak@ucf.edu

ABSTRACT

The impact of electron injection, using 10 keV beam of a Scanning Electron Microscope, on minority carrier transport in Si-doped β-Ga_2O_3 was studied for temperatures ranging from room to 120°C. *In-situ* Electron Beam-Induced Current technique was employed to determine the diffusion length of minority holes as a function of temperature and duration of electron injection. The experiments revealed a pronounced elongation of hole diffusion length with increasing duration of injection. The activation energy, associated with the electron injection-induced elongation of the diffusion length, was determined at ~ 74 meV and matches the previous independent studies. It was additionally discovered that an increase of the diffusion length in the regions affected by electron injection is accompanied by a simultaneous decrease of cathodoluminescence intensity. Both effects were attributed to increasing non-equilibrium hole lifetime in the valence band of β-Ga_2O_3 semiconductor.

I. INTRODUCTION

Wide bandgap semiconductors such as GaN and ZnO are important for a number of applications ranging from flame detection and high temperature electronics to solar-blind ultraviolet detectors and sensors for use in extreme environmental conditions.[1–3] An emerging semiconductor with a direct bandgap of 4.69 eV (ultra-wide bandgap), Ga_2O_3 has become an attractive candidate for radiation applications in terms of its superior stability over GaN and ZnO.[1,4–9]

So far, the main limiting factor in Ga_2O_3 technology is related to difficulties of p-type conductivity realization.[7,9–11] Previous studies indicate that holes in β-Ga_2O_3 have characteristics of low dispersion, high effective mass and high density of states. This results in formation of weak polarons (or localized holes), trapped by lattice distortions in the vicinity.[12–16] Contradicting these claims, Refs. 6 and 10 has recently experimentally shown a possibility of p-type conductivity in Ga_2O_3. It is additionally reported that the self-trapping nature of holes is destroyed at temperatures above 90-120 K.[11] Given the current state-of-the-art and ever mounting interest in p-type Ga_2O_3, one can reasonably claim that a robust p-type Ga_2O_3 electrical conductivity, if not yet fully feasible, will be possible in the foreseeable future.

In Ga_2O_3, if bipolar devices become available, minority carrier transport (diffusion length) will be of primary importance. Minority carrier diffusion length defines the performance of bipolar devices such as p-n junction diodes, bipolar transistors and p-*i*-n detectors.[6,9,17] One of the major issues in the current ZnO and GaN device technology, is the low diffusion length of minority carriers, partially due to dislocation scattering.[18,19] It has been previous shown that in p-type GaN and ZnO, electron injection either with an electron beam or forward bias, results in significant increase in minority carrier diffusion length.[18,20–23] Such an increase in the diffusion length translates into changes in the material's optical properties and improved photovoltaic detector performance.

Recent studies on diffusion length of minority holes in n-type β-Ga_2O_3 report the value ~ 400 nm at room temperature.[24,25] Hence, like in the case of ZnO and GaN, the issue of short diffusion length for minority carriers also exists in β-Ga_2O_3 and limits its possible applications in bipolar devices. This paper demonstrates the impact of electron injection on minority carrier transport in Si-doped β-Ga_2O_3. This study testifies that: 1) one can engineer minority carrier diffusion length with electron injection (increase it several times); 2) the non-equilibrium holes, generated due to electron beam, are not self-trapped and contribute profoundly to the Electron Beam-Induced Current.

II. EXPERIMENTAL

Electron Beam-Induced Current (EBIC) and Cathodoluminescence (CL) techniques[3,18,20–23] were employed *in-situ* in Philips XL30 Scanning Electron Microscope (SEM) to study the effect of electron injection on minority carrier transport, namely, diffusion length (L) and lifetime (τ) in β-Ga_2O_3. The samples involved in the study consisted of epitaxial Si-doped β-Ga_2O_3 grown on Sn-doped β-Ga_2O_3 substrate. The epitaxial layer growth was carried out by Halide Vapor-Phase Epitaxy (HVPE), courtesy Novel Crystal Technology, and the Sn-doped β-Ga_2O_3 substrate with [001] orientation was grown by edge-defined film-fed method (Tamura Corporation, Japan). Hall measurements on the n^+- doped substrate showed a carrier concentration of ~ 2.2×10^{18} cm^{-3}. The initial thickness of epitaxially grown Si-doped (with electron concentration ~ 3.6×10^{16} cm^{-3}[24]) β-Ga_2O_3 layer was 20 μm, which was subsequently reduced to 10 μm after chemical-mechanical polishing. Schottky rectifiers were obtained by making Schottky contacts (Ni – 20 nm/Au – 80 nm) on the epitaxial Si-doped β-Ga_2O_3 layer with photolithography/liftoff technique, and Ohmic contact on the Sn-doped β-Ga_2O_3 substrate (Ti – 20 nm/Au – 80nm) by blanket evaporation over the entire back side of the substrate. The diameter of the top contacts, used for measurements, was 210 μm.

The diffusion length of minority carriers was determined using line-scan EBIC technique in the planar configuration[24,26–30] with electron beam energy of 10 keV (corresponding to the electron range of ~ 0.4 μm and the absorbed current of ~ 0.4 nA in the material) in the temperature range of 23-120 °C (hot-stage of Gatan MonoCL2 system, integrated with Philips SEM, was used for varying temperature). A single line-scan, carried out from the edge of the Schottky barrier outwards (cf. Fig. 1, top-right inset), takes about 6 seconds. While L values can be extracted from this single line-scan, in this work, a scanning of the region of interest was not interrupted and was continued for a total duration of electron injection up to 720 seconds with periodic L measurements. Since this material was very sensitive to electron injection, the measurements for various temperatures were done at different locations, to exclude any possibility of uncalibrated electron injection. Line-scans were recorded using a home-made software interfaced with Stanford Research Systems Low-Noise Current Amplifier (SR570) and Keithley DMM 2000 digital multimeter.

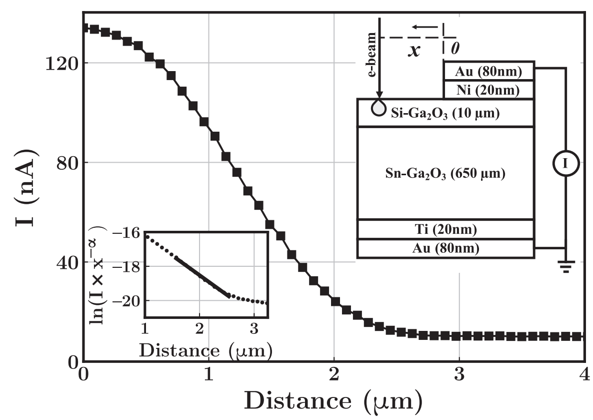

FIG. 1. A sample EBIC line-scan (*I* vs. distance) taken at room temperature. The distance is measured from the edge of the Schottky barrier and the fit is determined according to the equation (1). **Inset (top-right):** Schematic diagram of the measurement setup, **(bottom-left):** Linear fit according to the equation (2).

Variable-temperature CL measurements were carried out using Gatan MonoCL2 attachment to the SEM and an integrated temperature controller with an accuracy of 0.5 °C. The CL spectra were recorded with a single grating (1200 lines/mm blazed at 500 nm) monochromator and a Hamamatsu photomultiplier tube, sensitive in the 150-850 nm range. SEM electron beam with energy of 10 keV was used for excitation of 1 μm x 1 μm area, located at 10 μm distance from the Schottky contact, for a total electron injection duration of 3000 seconds.

III. RESULTS

The material was first analyzed at "zero" electron injection dose before studying the impact of electron injection. A single line-scan of 6 seconds was used, which had virtually no impact on L. A typical EBIC line-scan taken at room temperature is shown in Fig. 1, where the current is shown as a function of beam position measured from the edge of the Schottky contact.

L was extracted from the experimental data in Fig. 1 using the following equation:[27,29,31–33]

$$I(x) = I_0 x^{\alpha} \exp\left(-\frac{x}{L}\right), \tag{1}$$

where, x is the beam-to-junction distance, I_0 is a scaling constant, L is the diffusion length of minority carriers (holes, in this case), and α represents a surface recombination velocity and takes values between -1/2 and -3/2. Equation (1) is true for $x >> d$, where d is the depletion region width. Width of the depletion region is calculated as $d = [2\varepsilon\varepsilon_r(V_{bi}-V)/(qN_B)]^{0.5}$, where ε_r is the relative permittivity, V is the applied voltage, V_{bi} is the Schottky barrier built-in potential, q is the electron charge, and N_B is the bulk doping level in β-Ga_2O_3. In this case, ε_r=10.5,[1] V_{bi}=1.025 V,[34] V=0 V, and $N_B=3.6\times10^{16}$ cm^{-3}, resulting in $d \approx 179$ nm, which is at least 8 times less than x.

In equation (1), I_0, α, and L are fit parameters, and the fit was performed at the knee region of the curve in Fig. 1, which ensures the accuracy of the extracted parameters according to the constraint $x > 2L$.[31,35] Moreover, a modified form of equation (1), given below, reduces the three-parameter non-linear fit to a linear one, as shown in the bottom-left inset of Fig. 1:

$$\ln(I(x) \times x^{\alpha}) = -\frac{x}{L} + \ln(I_0) \tag{2}$$

L was calculated as the inverse slope of the linear fit according to equation (2). The best linear fit was obtained for $\alpha = -3/2$, which is, therefore, used throughout the article.

Temperature dependence of the L is given by:[32]

$$L(T) = L_0 \exp\left(\frac{\Delta E_{A,T}}{2kT}\right), \tag{3}$$

where k is the Boltzmann constant, L_0 is the asymptotic diffusion length, and T is the temperature in Kelvin. $\Delta E_{A,T}$ is the activation energy associated with a charge trap in the forbidden gap.[32] Temperature dependence of L is shown in Fig. 2. Similar to the previously reported results,[25] L exhibits a decrease from ~ 430 nm at room temperature to ~ 320 nm at 120 °C.

The decrease in L with temperature is not commonly observed in other semiconductors. In GaAs, ZnO and GaN, for example, L increases with temperature.[3,18,31] The activation energy, estimated from the Arrhenius plot (Fig. 2, inset) using equation (2), is ~ 53 meV. This energy is most likely associated with Si-donors, which form fairly shallow 50 meV levels.[36,37] A likely cause for L reduction with growing temperature could be related to thermalization of carriers.[38] Carrier-carrier interaction significantly contributes to thermalization only for high carrier concentrations (> $1\text{x}10^{18}$ cm^{-3}). For elevated temperatures and relatively low doping levels, such as in this case, carrier-phonon interaction becomes a dominating factor,[39,40] which leads to L decrease.

Continuous exposure of the sample to electron beam resulted in a significant x4.5 increase in L as shown in Fig. 3.

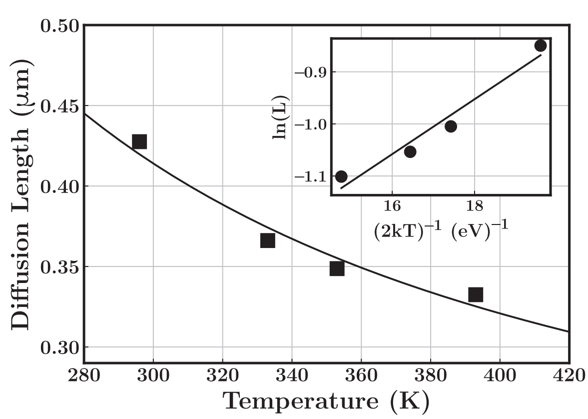

FIG. 2. Dependence of hole diffusion length on temperature for a single EBIC line-scan. **Inset:** The slope of the linear fit using equation (3) gives the thermal activation energy $\Delta E_{A,T}$ for the temperature dependence of diffusion length.

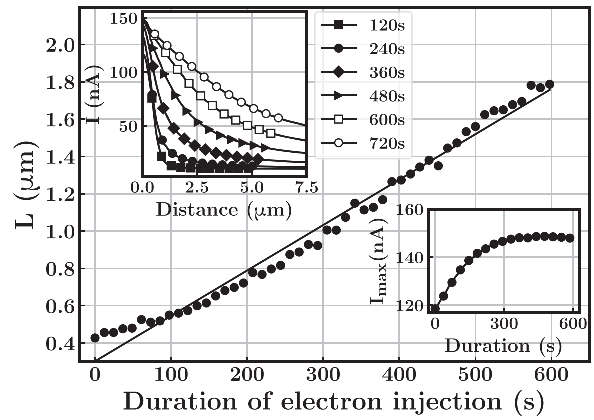

FIG. 3. Linear increase in the diffusion length due to continuous electron beam irradiation. **Inset (top):** Electron Beam Induced-Current vs. distance line-scans at various durations of electron injection. **Inset (bottom):** EBIC signal amplitude as a function of electron injection duration.

A similar effect was also observed in p-type ZnO and GaN as reported previously.[18,21] Fig. 3 (top inset) shows the EBIC line-scans for repeated exposures up to 720 seconds. A clear elongation (tail) is observed in the EBIC signal decay (compare a line-scan after 120 and 720 seconds of continuous electron beam excitation). As can be seen from equation (1), a longer tail in the EBIC signal dependence on distance, manifests in longer minority carrier diffusion length. A marked increase in the amplitude of the EBIC signal is also observed at the same time (cf. top and bottom insets of Fig. 3). The increase in the EBIC signal amplitude is attributed to the rise of the collection efficiency of minority carriers: longer L results in larger number of non-equilibrium minority electrons swept by built-in field of the Schottky barrier used in the measurements. The EBIC collection efficiency increases up to a certain value of L, after which any increase in L (which slows down with electron injection duration; cf. Fig.3, top inset) has no effect on the EBIC signal amplitude.[41–43] The diffusion length in Fig. 3 exhibits a saturation (not shown on the plot), following a saturation of I_{max} (cf. Fig. 3, bottom inset). It should be noted that the increased values of L, achieved due to electron beam injection, persist for at least one day at room temperature following injection.

Fig. 4 shows the effect of moderate electron injection duration on minority carrier diffusion length. This study was carried out at variable temperature to understand its impact on the rate of L increase (μm/sec) due to electron injection. The plot for room temperature in Fig. 4 can be correlated with the 0-100 second segment of L versus electron injection duration in Fig. 3, with a slight mismatch in slope attributed to different locations for two experiments.

The effect of temperature on the rate, R, of L increase with electron injection duration can be described as:[18]

$$R(T) = R_0 \exp\left(\frac{\Delta E_{A,T}}{2kT}\right) \exp\left(\frac{\Delta E_{A,I}}{kT}\right), \tag{4}$$

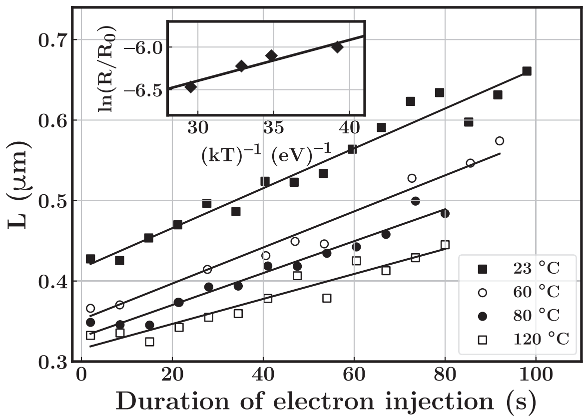

FIG. 4. Temperature dependence for minority hole diffusion length increase due to electron injection. The rate, R, of diffusion length elongation decreases with temperature. **Inset:** The slope of the linear fit with equation (4) giving the activation energy $\Delta E_{A,I}$ for the electron injection-induced increase of L.

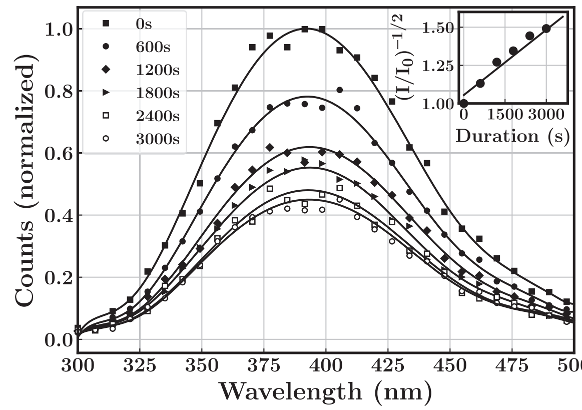

FIG. 5. CL spectra from the region affected by electron injection as a function of its duration. **Inset:** Dependence of the square root for normalized (relative to the maximum intensity I_0) inversed intensity on duration of electron injection, and the linear fit.

where R_0 is a constant, $\Delta E_{A,T}$ is thermal activation energy for diffusion length (from equation (3)), and $\Delta E_{A,I}$ is the activation energy due to electron injection effect.

As R implicitly contains the injection information in the form of L versus electron injection duration, t ($R=dL/dt$), use of equation (4) to calculate $\Delta E_{A,I}$ is justified. In equation (4), the first exponent represents L dependence on temperature (cf. equation (3), in which a $\frac{1}{2}$ factor in the exponent is due to equation (5) (see below)); the second exponent is a Boltzmann factor, which is used to model the temperature dependence of electron injection effect. One can see from Fig. 4 that R decreases with increasing temperature. Fig. 4 (inset) shows the Arrhenius plot with a linear fit of R vs. $1/kT$, according to equation (4), yielding $\Delta E_{A,I}$ to be ~ 74 meV. Similar activation energy, attributed to yet unknown recombination center, was recently observed in an independent study.[44]

The diffusion length of minority carriers is an integral quantity, which is related to the lifetime of non-equilibrium carriers in the band by the relation:[19]

$$L = \sqrt{D\tau}, \tag{5}$$

where D is the diffusion coefficient and τ is the minority carrier lifetime. A larger lifetime of non-equilibrium carriers in the band indicates lower number of radiative recombination events.[45] If L increase is due to an increase in τ, the CL intensity from the radiative recombination process should decrease with duration of electron injection. Indeed, from the CL experiment performed at room temperature (Fig. 5), a decrease in the CL intensity I, was observed with the duration of electron injection.

Earlier studies have shown that $I^{-1} \propto \tau$.[45] Moreover, L depends linearly on electron injection duration (Figs. 3, 4) and on $\sqrt{\tau}$ (equation (5)). Hence, it is concluded that the dependence of CL intensity on electron injection duration, t, should be given by $I^{-1/2} \propto t$.[45] This relation was verified by the linear fit in Fig. 5, inset, which is also in agreement with the assumption that the linear increase of L with injection duration is due to an increased lifetime for minority carriers.

IV. DISCUSSION AND CONCLUSIONS

The proposed model for the observed electron injection-induced effects in β-Ga_2O_3 is as follows:

- Non-equilibrium electron-hole pairs are generated in β-Ga_2O_3 due to electron beam irradiation. The total charge, injected into the region under investigation due to this irradiation, is up to 1.2 μC.
- We expect that the unknown traps with activation energy of 74 meV (see above) can capture some non-equilibrium electrons. A similar situation was observed in Mg-doped GaN and Sb-doped ZnO.[3,18,21–23]
- As a portion of non-equilibrium electrons is captured, these traps stop playing a role in the recombination process (mostly radiative, cf. Fig. 5) and the non-equilibrium electrons and holes live longer life (τ) in the conduction and valence bands, respectively. Increased τ leads to longer minority carrier diffusion length L (as measured by EBIC) and suppressed CL intensity from the region subjected to electron irradiation (cf. Fig. 5). As the electron injection continues, the number of traps, available to capture non-equilibrium electrons, saturates. As a result, the EBIC signal amplitude (cf. insets of Fig. 3) and the CL intensity (cf. Fig. 5) reach their saturation levels.
- As the temperature increases, trapped electrons have a higher chance to escape and recombine with holes in the valence band. At the same time, the traps again become available for recombination. This leads to a reduced rate R (for L increase with electron irradiation duration) at elevated temperatures (cf. Fig. 4).

In conclusion, this study demonstrates a significant increase of minority hole diffusion length in n-type β-Ga_2O_3.

Enhancement of minority carrier transport is accompanied by the consistent changes in the material's optical properties. Both effects are related to an increased lifetime for non-equilibrium carriers in the conduction and valence bands (non-equilibrium electrons and holes are generated in pairs). Additionally, the experiments show that minority holes may substantially contribute to current in β-Ga_2O_3 semiconductor, which is an argument against self-trapping at room and elevated temperatures.

ACKNOWLEDGMENTS

Research at UCF and the Weizmann institute was supported in part by NATO (award # G5453) and NSF (UCF award # ECCS1802208). The work at UF was sponsored by the Department of Defense, Defense Threat Reduction Agency, HDTRA1-17-1-011, monitored by Jacob Calkins.

REFERENCES

[1]S. J. Pearton, J. Yang, P. H. Cary, F. Ren, J. Kim, M. J. Tadjer, and M. A. Mastro, Applied Physics Reviews **5**, 011301 (2018).
[2]J. V. Li, S. L. Chuang, E. M. Jackson, and E. Aifer, Appl. Phys. Lett. **85**, 1984 (2004).
[3]L. Chernyak, A. Osinsky, and A. Schulte, Solid-State Electron. **45**, 1687 (2001).
[4]A. Y. Polyakov, N. B. Smirnov, I. V. Shchemerov, S. J. Pearton, F. Ren, A. V. Chernykh, and A. I. Kochkova, Appl. Phys. Lett. **113**, 142102 (2018).
[5]H. Gao, S. Muralidharan, N. Pronin, M. R. Karim, S. M. White, T. Asel, G. Foster, S. Krishnamoorthy, S. Rajan, L. R. Cao, M. Higashiwaki, H. von Wenckstern, M. Grundmann, H. Zhao, D. C. Look, and L. J. Brillson, Appl. Phys. Lett. **112**, 242102 (2018).
[6]J. Yang, F. Ren, S. J. Pearton, G. Yang, J. Kim, and A. Kuramata, Journal of Vacuum Science & Technology B, Nanotechnology and Microelectronics: Materials, Processing, Measurement, and Phenomena **35**, 031208 (2017).
[7]A. Mock, R. Korlacki, C. Briley, V. Darakchieva, B. Monemar, Y. Kumagai, K. Goto, M. Higashiwaki, and M. Schubert, Phys. Rev. B **96**, 245205 (2017).
[8]M. A. Mastro, A. Kuramata, J. Calkins, J. Kim, F. Ren, and S. J. Pearton, ECS Journal of Solid State Science and Technology **6**, P356 (2017).
[9]S. I. Stepanov, V. I. Nikolaev, V. E. Bougrov, and A. E. Romanov, Rev. Adv. Mater. Sci. **44**, 63 (2016).
[10]E. Chikoidze, A. Fellous, A. Perez-Tomas, G. Sauthier, T. Tchelidze, C. Ton-That, T. T. Huynh, M. Phillips, S. Russell, M. Jennings, B. Berini, F. Jomard, and Y. Dumont, Materials Today Physics **3**, 118 (2017).
[11]B. E. Kananen, N. C. Giles, L. E. Halliburton, G. K. Foundos, K. B. Chang, and K. T. Stevens, J. Appl. Phys. **122**, 215703 (2017).
[12]J. B. Varley, A. Janotti, C. Franchini, and C. G. Van de Walle, Phys. Rev. B **85** (2012).
[13]S. Yoshioka, H. Hayashi, A. Kuwabara, F. Oba, K. Matsunaga, and I. Tanaka, J. Phys.: Condens. Matter **19**, 346211 (2007).
[14]H. He, R. Orlando, M. A. Blanco, R. Pandey, E. Amzallag, I. Baraille, and M. Rérat, Phys. Rev. B **74**, 195123 (2006).
[15]H. He, M. A. Blanco, and R. Pandey, Appl. Phys. Lett. **88**, 261904 (2006).
[16]J. Furthmüller and F. Bechstedt, Phys. Rev. B **93**, 115204 (2016).
[17]M. Higashiwaki, K. Konishi, K. Sasaki, K. Goto, K. Nomura, Q. T. Thieu, R. Togashi, H. Murakami, Y. Kumagai, B. Monemar, A. Koukitu, A. Kuramata, and S. Yamakoshi, Appl. Phys. Lett. **108**, 133503 (2016).
[18]O. Lopatiuk-Tirpak, L. Chernyak, F. X. Xiu, J. L. Liu, S. Jang, F. Ren, S. J. Pearton, K. Gartsman, Y. Feldman, A. Osinsky, and P. Chow, J. Appl. Phys. **100**, 086101 (2006).
[19]L. Chernyak, A. Osinsky, G. Nootz, A. Schulte, J. Jasinski, M. Benamara, Z. Liliental-Weber, D. C. Look, and R. J. Molnar, Appl. Phys. Lett. **77**, 2695 (2000).
[20]L. Chernyak, G. Nootz, and A. Osinsky, Electron. Lett. **37**, 922 (2001).
[21]L. Chernyak, A. Osinsky, V. Fuflyigin, and E. F. Schubert, Appl. Phys. Lett. **77**, 875 (2000).
[22]O. Lopatiuk-Tirpak, L. Chernyak, Y. L. Wang, F. Ren, S. J. Pearton, K. Gartsman, and Y. Feldman, Appl. Phys. Lett. **90**, 172111 (2007).
[23]O. Lopatiuk-Tirpak, L. Chernyak, L. J. Mandalapu, Z. Yang, J. L. Liu, K. Gartsman, Y. Feldman, and Z. Dashevsky, Appl. Phys. Lett. **89**, 142114 (2006).
[24]E. B. Yakimov, A. Y. Polyakov, N. B. Smirnov, I. V. Shchemerov, J. Yang, F. Ren, G. Yang, J. Kim, and S. J. Pearton, J. Appl. Phys. **123**, 185704 (2018).
[25]J. Lee, E. Flitsiyan, L. Chernyak, J. Yang, F. Ren, S. J. Pearton, B. Meyler, and Y. J. Salzman, Appl. Phys. Lett. **112**, 082104 (2018).
[26]O. Kurniawan and V. K. S. Ong, 2006 Conference on Optoelectronic and Microelectronic Materials and Devices, IEEE, Perth, WA, Australia (2006).
[27]D. E. Ioannou and C. A. Dimitriadis, IEEE Trans. Electron Devices **29**, 445 (1982).
[28]C. A. Dimitriadis, Journal of Physics D-Applied Physics **14**, 2269 (1981).
[29]F. Berz and H. K. Kuiken, Solid-State Electron. **19**, 437 (1976).
[30]L. Jastrzebski, J. Lagowski, and H. C. Gatos, Appl. Phys. Lett. **27**, 537 (1975).
[31]L. Chernyak, A. Osinsky, H. Temkin, J. W. Yang, Q. Chen, and M. Asif Khan, Appl. Phys. Lett. **69**, 2531 (1996).
[32]M. Eckstein and H. U. Habermeier, J. Phys. IV **1**, 23 (1991).
[33]H. J. Leamy, J. Appl. Phys. **53**, R51 (1982).
[34]J. Yang, C. Fares, R. Elhassani, F. Ren, S. J. Pearton, M. Tadjer, and A. Kuramata, Unpublished Results (2018).
[35]D. S. H. Chan, V. K. S. Ong, and J. C. H. Phang, IEEE Trans. Electron Devices **42**, 963 (1995).
[36]H. Masataka, K. Akito, M. Hisashi, and K. Yoshinao, J. Phys. D: Appl. Phys. **50** (2017).
[37]A. T. Neal, S. Mou, S. Rafique, H. Zhao, E. Ahmadi, J. S. Speck, K. T. Stevens, J. D. Blevins, D. B. Thomson, N. Moser, K. D. Chabak, and G. H. Jessen, Appl. Phys. Lett. **113**, 062101 (2018).
[38]P. Yu and M. Cardona, *Fundamentals of Semiconductors: Physics and Materials Properties* (Springer Berlin Heidelberg, 2010).
[39]T. Onuma, S. Saito, K. Sasaki, K. Goto, T. Masui, T. Yamaguchi, T. Honda, A. Kuramata, and M. Higashiwaki, Appl. Phys. Lett. **108**, 101904 (2016).
[40]N. Ma, N. Tanen, A. Verma, Z. Guo, T. Luo, H. Xing, and D. Jena, Appl. Phys. Lett. **109**, 212101 (2016).
[41]M. Ledra and N. Tabet, Superlattices and Microstructures **45**, 444 (2009).
[42]E. B. Yakimov, S. S. Borisov, and S. I. Zaitsev, Semiconductors **41**, 411 (2007).
[43]C. Donolato, Journal de Physique Colloques **50**, 57 (1989).
[44]T. T. Huynh, L. L. C. Lem, A. Kuramata, M. R. Phillips, and C. Ton-That, Physical Review Materials **2** (2018).
[45]L. Chernyak, W. Burdett, M. Klimov, and A. Osinsky, Appl. Phys. Lett. **82**, 3680 (2003).